Article

Ytterbium-Doped Double-Clad Fiber with High Uniformity of Concentration Distribution and Suppressed Photodarkening

Yongqing Yi, Yize Shen, Pengcheng Geng, Rong Pan, Shijie Xu * and Ruifang Luo

Tianjin Key Laboratory of Special Optical Fiber Materials, The 46th Research Institute, China Electronics Technology Group Corporation, Tianjin 300220, China; yiyongq@126.com (Y.Y.); kimisyzcxy@163.com (Y.S.); gengpengcheng@126.com (P.G.); pprr-0305@163.com (R.P.); luoruifang001@163.com (R.L.)
* Correspondence: xusj2023@163.com

Abstract: Photodarkening (PD) effect in ytterbium-doped fiber (YDF) has a significant impact on the high-power operational stability of fiber lasers, which seriously hinders the power scaling. In this paper, the relationship between ytterbium ions uniformity and the photodarkening effect in the YDF was investigated, and the fabrication process allowing improving the ytterbium ions uniformity in the core of preforms for suppressing the photodarkening effect was developed. The Modified Chemical Vapor Deposition (MCVD) method combined with Chelate Vapor Deposition (CVD) technology was adopted for multi-layer fiber core deposition, and an all-gas-phase technical process was proposed to improve the ytterbium ions uniformity in the Al/P co-doped glass matrix. The $25/400~\mu m$ YDFs obtained by this technology achieved stable 3.5 kW laser output power for 8 h with suppressed PD and nonlinear effects.

Keywords: ytterbium-doped double-clad fiber; ytterbium ion uniformity; photodarkening effect; multilayer gradient deposition

1. Introduction

Because of its high stability, high beam quality and slope efficiency, the ytterbium-doped double-clad fiber laser has a wide range of applications in industrial processing, advanced manufacturing and other fields [1,2]. However, as the operating time of high-power fiber lasers extends, the output power decreases due to the increasing fiber loss, i.e., the photodarkening (PD) effect. The PD effect manifests an increase in loss in broadband centered at visible wavelengths. The excess loss caused by the PD effect will influence pumping absorption and emission in Yb-doped fibers. The PD effect reduces system stability and shortens operating time, which limits the further development of ytterbium-doped fiber lasers [3–7].

Many researchers are focused on revealing the PD mechanism. The oxygen deficiency center (ODC), charge transfer absorption band and Tm impurities are three reasonable explanations for the generation of PD [8–10].

PD can be suppressed at the point of its generation (i.e., active inhibition) or mitigated after fiber fabrication (i.e., passive inhibition). Multiple fiber glass compositions have been employed to suppress PD from the point of generation (Al, Ce, P, Na, Mg, Ca, etc.) [11–21]. Differences in these doping systems have been analyzed. The photodarkening-induced excess losses of Yb/Al/Ce co-doped fiber at chosen wavelengths were more than double those of Yb/Al/P co-doped fiber [22]. Yb/Al-doped silica fibers with high Al concentrations exhibited negligible photodarkening levels, even with significantly higher Yb concentrations than those typically used in commercial Yb-doped silica fibers [23,24]. Furthermore, special fiber structure designs and fabrication methods can also suppress PD from the point of generation [25–28].

The PD effect generated during fabrication can be mitigated by the subsequent processing of the fiber. The processing methods include photobleaching [5,29], thermal bleach-

ing [30], gas loading [31,32], etc. The purpose of these methods is to mitigate the impact of PD on the properties of fibers. Nonetheless, the efficacy of these methods is often dictated by the concentration and inhomogeneity of Yb ion.

In this paper, ytterbium-doped double-clad fiber was obtained by the MCVD method combined with the CVD deposition process, and the doping uniformity of ytterbium ions in the core of the fiber was effectively improved by fine-tuning the proportion of the core glass components layer-by-layer through the technical process optimization. A 25/400 μm ytterbium-doped double-clad fiber with a top-flatten refractive index profile (RIP) was developed based on the fabricated fiber. The MOPA test system was built to achieve 3482 W laser output power under 4025 W pump power. No Raman effect was observed, and the laser continued to work for 8 h without noticeable output power reduction. By experimental study, it is proved that more attention should be paid to the uniformity of ytterbium ions doping in the fiber core, and the technology plays an important role in suppressing the PD effect, allowing for higher and stable output power.

2. Theory of the Effect of Core Doping Uniformity on Photodarkening

In order to suppress the nonlinear effect in a fiber laser, a high concentration of ytterbium ions is needed to achieve a ytterbium-doped fiber with high output power. However, during the fabrication process, there is a risk of an uneven distribution of ytterbium ion concentration in fibers fabricated via MCVD combined with either the solution-doping method or the chelate vapor-doping method. The Yb/Al/P co-doped system was adopted for its superior PD resistance and high threshold of transverse mode instability (TMI) [22]. The main reason for the non-uniformity of ytterbium ions' distribution in the core can be described as follows. After depositing and drying, the silica tube is sintered at 1800~2100 °C and collapses at 2200~2300 °C. The main dopants in the fiber are P_2O_5, Al_2O_3 and Yb_2O_3. Among these dopants, P_2O_5 has the lowest volatilizing temperature, while Al_2O_3 and Yb_2O_3 have higher volatilizing temperatures. P_2O_5 will volatilize because of the high temperature at the point of collapse. In the silica network, chemical bonds form between P_2O_5, Al_2O_3 and Yb_2O_3. As the P_2O_5 volatilizes, the chemical bonds between P_2O_5, Al_2O_3 and Yb_2O_3 break up. At the same time, some of the Al_2O_3 and Yb_2O_3 will be taken away, which leads to non-uniformity in the concentration distribution. As a result, although Al and Yb oxides are not volatile compounds, non-uniformity arises in the concentration distribution.

For fibers with non-uniform ytterbium ion distribution, there will be large concentration differences between the areas with the highest and the lowest concentration. It is easier for oxygen vacancy defects to form in local areas with relatively high concentrations of ytterbium ions. In Yb-doped fibers, oxygen vacancy defects can lead to photodarkening effects. As a result, the non-uniformity of ytterbium ion distribution causes photodarkening in a Yb-doped fiber.

The ytterbium ion distribution influences both efficiency and the photodarkening effect. It has been proven that the degree of population inversion of the ytterbium ion has a strong influence on the photodarkening effect [33]. Higher population inversion of the ytterbium ions causes higher excess loss of photodarkening induced in the same pump time range, which means the output power decays more rapidly. According to the fiber laser rate equation, under circumstances without strong spontaneous emission light amplification, the degree of population inversion can be expressed as follows [34]:

$$n_2 = \frac{\sigma_{ap} I_p}{\sigma_{ap} I_p + \sigma_{ep} I_p + \frac{1}{\tau}} \tag{1}$$

In the expression, n_2 represents the degree of population inversion; σ_{ap} and σ_{ep} represent the absorption and emission cross-sections of the fiber, respectively; I_p represents the incident pump intensity and τ represents the fluorescence lifetime. It can be seen from the expression that the population inversion of ytterbium ions is related to the absorption and emission cross-sections of the fiber for a constant pump intensity. The non-uniform distribution results in a greater difference between the absorption and emission cross-

sections and a higher degree of ytterbium ion population inversion, thus inducing a greater photodarkening excess loss and a reduced laser output power.

In addition, the non-uniformity of the concentration distribution leads to a difference in temperature distribution inside the fiber, which causes various degrees of thermal expansion in the inner and outer layers of the material, resulting in different thermal stresses in the radial, tangential and axial directions. We found that high laser efficiency, kilowatt laser power and long-term output stabilization can be achieved using fiber with high uniformity in the ytterbium ion distribution. On the contrary, for a fiber with low doping uniformity, the laser efficiency of the fiber is relatively low and the output power does not reach the kilowatt order.

3. Preform Fabrication and Test

With the capacity to preform optical fibers with good doping uniformity, MCVD combined with the chelate vapor deposition process was adopted for fabrication in our experiment.

In order to improve the uniformity of Yb concentration distribution, a multi-layer gradient deposition technique was adopted. According to the correspondence between the refractive index distribution and concentrations of different elements in the core, and the laws of diffusion and volatilization of different components in the core at high temperatures, the doping flows of Al, P and other elements were fine-tuned layer by layer. The doping uniformity was effectively improved by adjusting the flow, doping concentration and deposition thickness, so as to control the refractive index distribution and the concentration distribution of the core elements. After theoretical analyses and extensive experimental studies, the final parameters of the multilayer deposition process of the 25/400 Yb-doped double-clad fiber were determined, as shown in Table 1. Layer 1 is the first deposition layer, which forms the boundary of the core, while Layer 7 is the last deposition layer which forms the center of the core.

Table 1. Process parameters of multilayer deposition.

Flow (sccm)	Layer 1	Layer 2	Layer 3	Layer 4	Layer 5	Layer 6	Layer 7
$AlCl_3$	95	98	100	103	105	110	110
$POCl_3$	80	80	85	90	95	100	105
$Yb(thd)_3$	400	400	400	405	408	410	412

The concentration inhomogeneity was suppressed by increasing the flow of $AlCl_3$, $POCl_3$ and $Yb(thd)_3$ layer by layer. The $AlCl_3$ flow was increased layer by layer from 95 sccm to 110 sccm with a 15% increment. The $POCl_3$ flow was increased layer by layer from 80 sccm to 105 sccm with a 31% increment. The high volatilizing ratio meant that the flow of $POCl_3$ showed the highest proportion of increase (~31%). The flow of $Yb(thd)_3$ was increased layer by layer from 400 sccm to 412 sccm, with a 3% increment.

It is obvious that $AlCl_3$, $POCl_3$ and $Yb(thd)_3$ showed different increments of flow from Layer 1 to Layer 7. The reasons for this are as follows: After the deposition of the seven-layer core is completed, it is necessary to collapse the reaction tube with gaps in the middle into a solid ytterbium-doped fiber preform, and the collapsing temperature of the reaction tube generally needs to reach 2200 °C or above. At such a high collapsing temperature, the volatilization of P_2O_5 caused by the reaction between $POCl_3$ and O_2 in the core layer of the preform will intensify, and the volatilization of P_2O_5 in the inner core layer will be more severe. So, the P_2O_5 in the seventh layer will volatilize the most severely, and that of the P_2O_5 in the sixth layer will be the second most severe. Due to the blocking of the inner core layers, the P_2O_5 in the second and first core layers will hardly evaporate. During deposition, the flow of $SiCl_4$ will be constant at 175 sccm and the deposition temperature will be 2050 °C in each layer. The temperatures of $AlCl_3$ and $Yb(thd)_3$ will be 143 °C and 217 °C, respectively.

The refractive index distribution of the preform was tested using PK2600 from the United States PK Company. Then, the preform was cut on one end in order to obtain a preform slice. The concentration distributions of Yb ions in the preform slices were tested using the preform slice analyzer from OPHIR, Israel, and an electronic probe (EPMA-1720) from Shimadzu, Japan.

4. Results and Discussion

4.1. Refractive Index and Concentration Distribution of Preform

Figure 1a,b show the refractive indices of the preform before optimization and after optimization, respectively. It can be seen from the result that the difference between the core-clad refractive indices was 0.0012, which corresponds to a numerical aperture (N.A.) of 0.06.
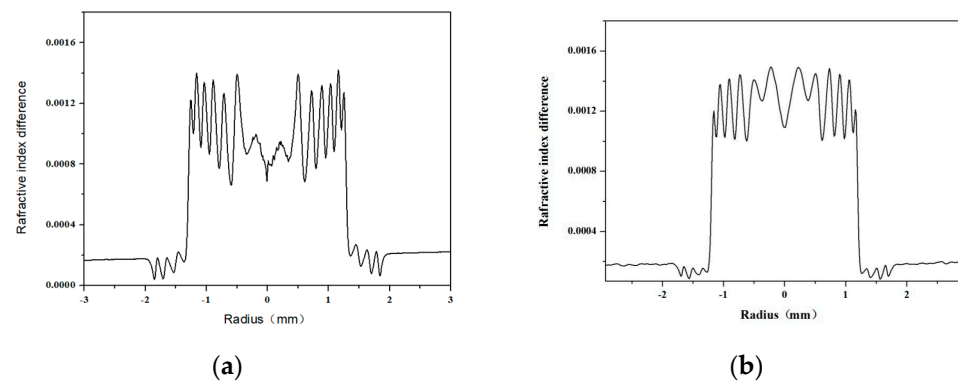

(**a**)   (**b**)

Figure 1. The refractive index difference of the preform: (**a**) before optimization and (**b**) after optimization.

The core refractive index distribution of the preform after optimization showed less fluctuation. There was a decline in the refractive index (~0.0004) in the center of the preform core before optimization. Meanwhile, the refractive index was flat in the center of the preform core after optimization, indicating the promotion of uniformity in the distribution of the doped elements in the fiber core.

The distributions of the concentrations of Yb ions in the preform core before and after optimization were tested using a preform slice analyzer, as shown in Figure 2. In Figure 2a,c, the Yb ion concentration is labeled with colors. In Figure 2b,d, the scan line passes through the core center, and the longitudinal axis represents the concentration of Yb ions.

It can be seen from Figure 2a,b that there was a dip in the concentration in the core center. In Figure 2c,d, we can see no dip in the center. To get all the required information and draw further conclusions, we need the contribution distribution of Al and P as well as Yb. The concentration distributions of dopant elements (Yb, Al and P) in the preform core before and after optimization were tested by EPMA, as shown in Figure 3.

Combining Figures 2 and 3, it is clear that in the sample before optimization, the concentrations of Yb, Al and P in the central area were lower than in the other areas in the fiber core. In the sample after optimization, the concentration in the central area was equal to that in other areas in the fiber core, indicating a substantial improvement in Yb, Al and P concentration distribution uniformity. We analyzed the reasons for this improvement. Before the improvement process, during the fabrication of ytterbium-doped fiber preforms, the deposition flow rates of each core layer were the same. This caused the severe volatilization of P_2O_5 in the seventh and sixth core layers during high-temperature collapsing, resulting in a decrease in the concentrations of Yb, Al and P in the center of the ytterbium-doped fiber core. After the process of improvement, during the preparation of ytterbium-doped fiber preforms, the deposition flow rate of each core layer was increased, as shown in Table 1.

This allowed us to achieve a relatively uniform concentration distribution of Yb, Al and P in the fiber core.

In order to analyze the concentration distribution quantitatively, the S-value of Yb ion concentration is used here to evaluate uniformity. The line scanning results for a regular preform slice measured by EPMA are shown in Figure 4.
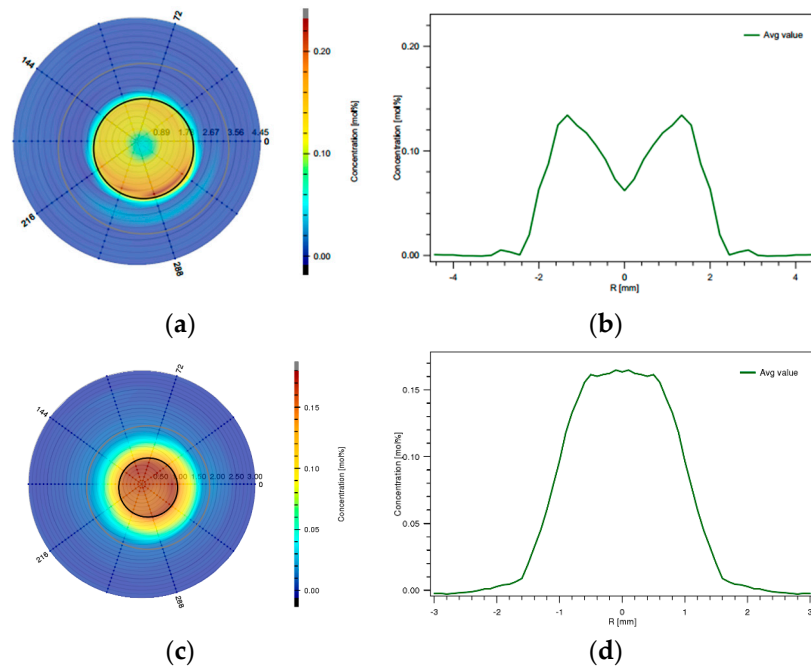

Figure 2. Concentration distribution of Yb (tested by preform slice analyzer): (**a**) surface scanning result before optimization, (**b**) line scanning result before optimization, (**c**) surface scanning result after optimization and (**d**) line scanning result after optimization.

The S-value of ytterbium ion concentration distribution refers to the standard deviation of concentration along the scanning line. The expression for the S-value is as follows:

$$S_\theta = \sqrt{\frac{1}{n}\sum_{i=1}^{n}(x_i - \overline{x})^2} \tag{2}$$

In the expression, S_θ refers to the S-value in direction θ, n refers to the number of points selected on the scanning line, x_i refers to the concentration of point i and $\overline{x}$ refers to the average concentration of the scanning line. A lower S-value represents the relatively better uniformity of Yb ion distribution. Table 2 presents the S-values of five preform slices with different concentration distributions (Sample 1 refers to the preform before optimization and experiments were performed on Samples 2~5). Three line scans were performed on each preform slice. The included angles of each line scanning direction were 120°. S_0, S_{120} and S_{240} refer to the S-values scanned at 0°, 120° and 240°, respectively. From the test data, it is apparent that an improvement in the uniformity of Yb concentration distribution was achieved in our experiment.

Table 2. Comparison of ytterbium ion distribution in the fiber core.

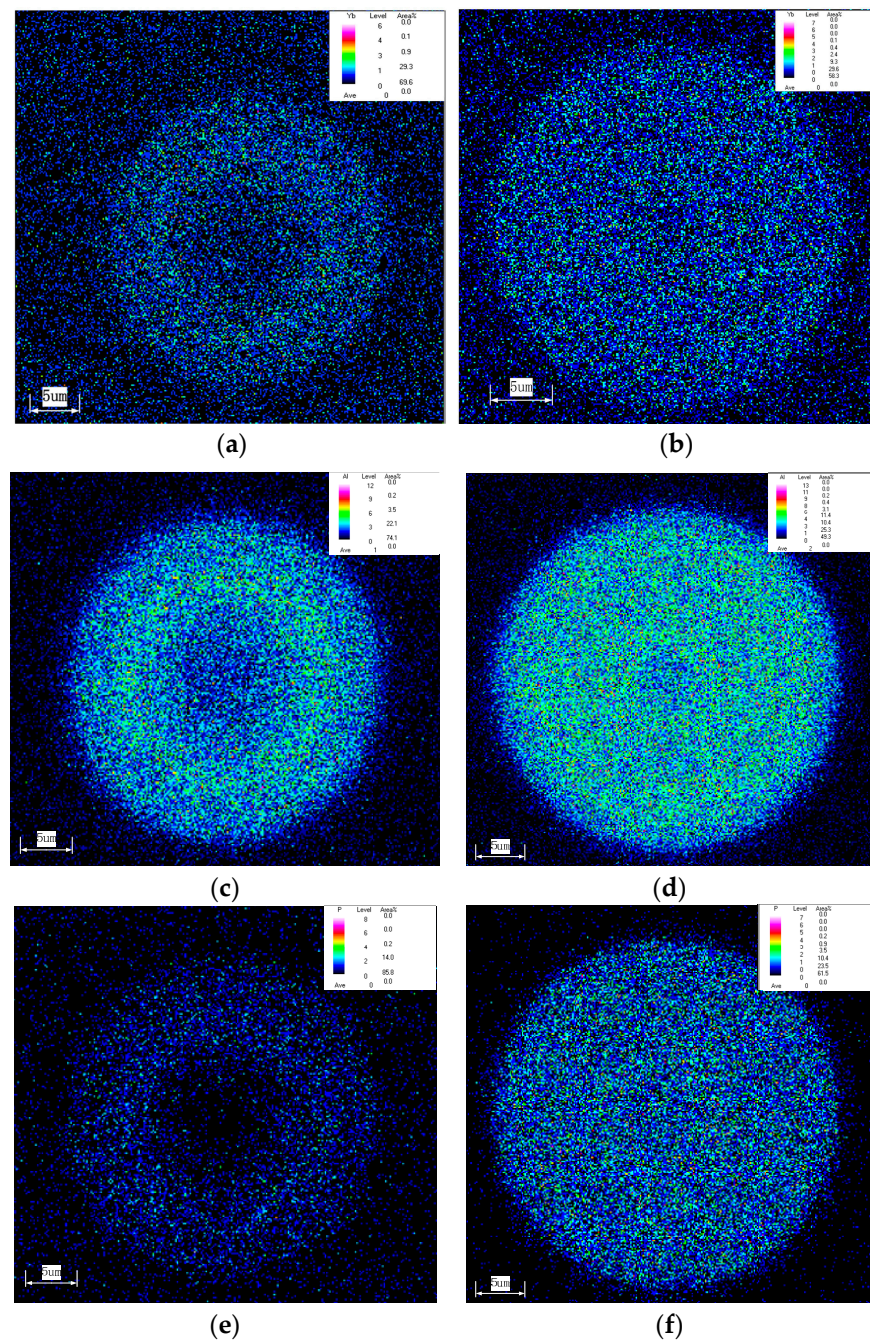|	Sample 1	Sample 2	Sample 3	Sample 4	Sample 5
S_0	0.420	0.203	0.104	0.010	0.001
S_{120}	0.448	0.295	0.122	0.008	0
S_{240}	0.397	0.121	0.089	0.008	0

Figure 3. Concentration distribution of dopant elements in the preform core (tested by EPMA): (**a**) concentration distribution of Yb before optimization, (**b**) concentration distribution of Yb after optimization, (**c**) concentration distribution of Al before optimization, (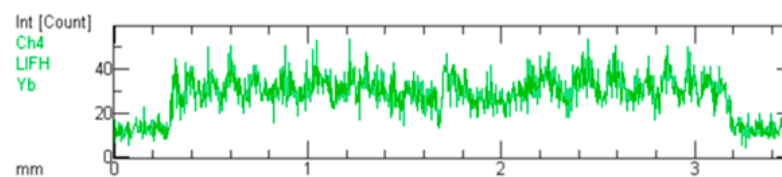**d**) concentration distribution of Al after optimization, (**e**) concentration distribution of P before optimization and (**f**) concentration distribution of P after optimization.

Figure 4. Line scanning result for a preform slice.

4.2. Fiber Optic Performance Testing

This paper investigates the relationship between the uniformity of distribution of various dopants and the PD effect via laser experiments. The preforms were drawn into optical fibers after testing. The laser output powers were obtained using an 800 W laser test platform, as shown in Figure 5.
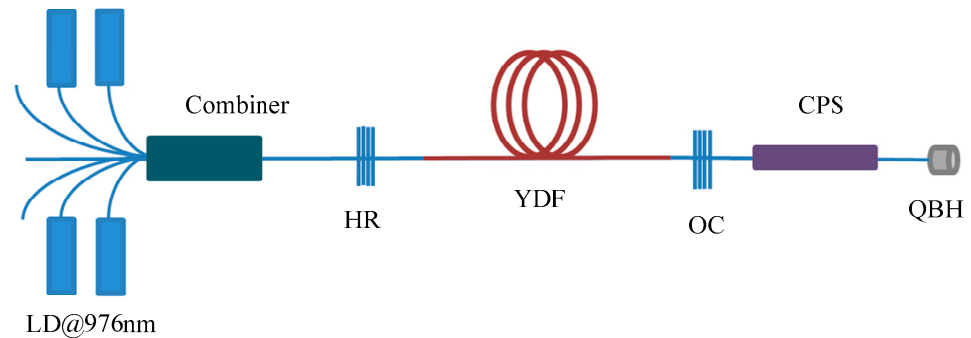

Figure 5. Schematic of 800 W fiber laser platform.

The laser outputs of Samples 2 to 5 are shown in Figure 6. The laser output of Sample 1 is not shown in Figure 6 because the laser output was unstable. The output power of Sample 2 declined rapidly after 500 W. The output power of Sample 3 declined rapidly after about 1 h of continuous operation at 610 W. The output power of Sample 4 declined slowly after about 3 h of continuous operation at 660 W. The output power of Sample 5 was stable for 10 h without a reduction at 680 W.
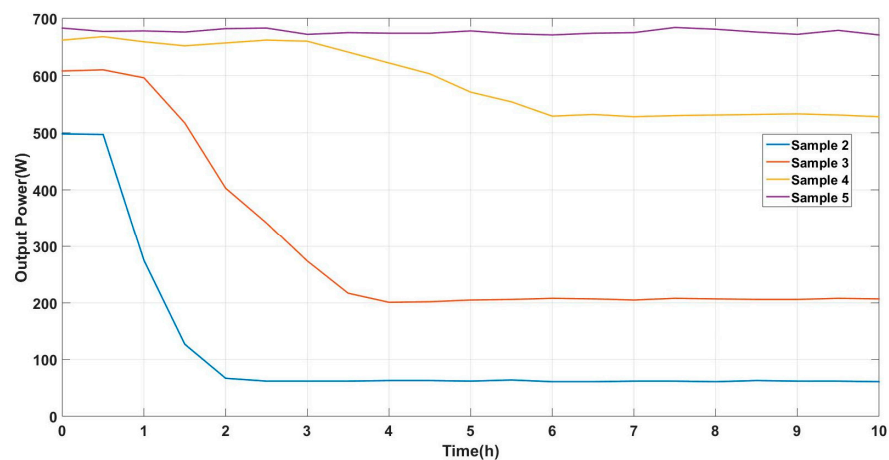

Figure 6. The output power of fibers with different Yb concentration distributions.

As illustrated in Figure 6, Sample 5 demonstrated a consistent laser output power of 680 W over an extended duration, in contrast to the varying degrees of stability observed in the power levels of other samples, which demonstrated a suppression of photodarkening. This result could be explained by the promotion of homogeneity in the internal temperature distribution. When the laser is generated in the fiber core, heat is generated at the same time. With the promotion of homogeneity in the concentration distribution, the internal temperature distribution became more uniform. As a result, the accumulation of thermal effects was mitigated, and any subsequent photodarkening was suppressed.

Of note, the high degree of population inversion typically observed in high-concentration areas within the core did not occur in this instance. This absence resulted in the suppression of any excess loss of photodarkening, allowing the laser to maintain a stable output of 680 W. These findings underscore the critical importance of uniform concentration distribution and thermal management in optimizing the performance of such fibers.

The geometric dimensions and optical performance of Sample 5 were measured. The end face of the optimized Yb-doped double-clad fiber prepared via the optimization method is shown in Figure 7, with a core diameter of 24.6 μm and an inner cladding (side-to-side) diameter of 401.1 μm. The absorption coefficient of the Yb-doped double-clad fiber was measured via the truncation cutoff method, and the results are shown in Figure 8, with a cladding absorption coefficient of 2.45 dB/m at 976 nm.
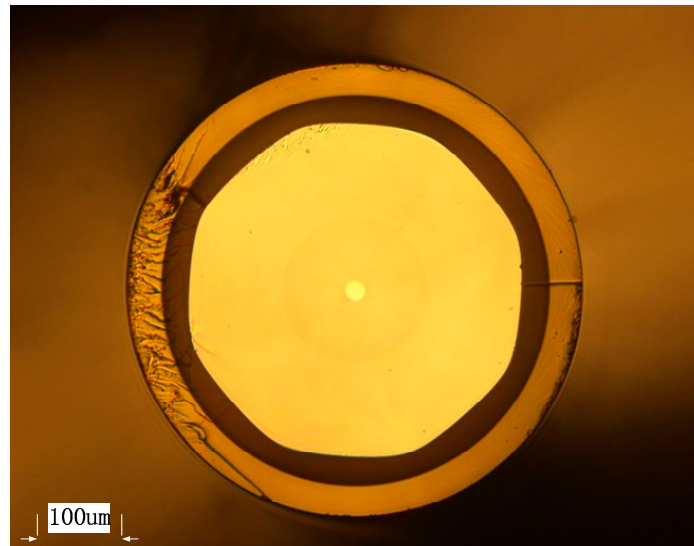
Figure 7. The cross-section of the 25/400 μm Yb-doped fiber.

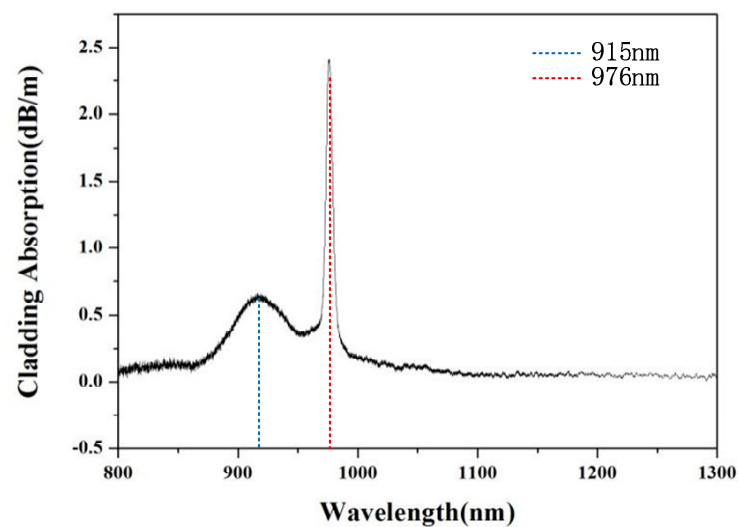**Figure 8.** The cladding absorption of the Yb-doped fiber.

Since the core diameter of the Yb-doped double-clad fiber is 25 μm, a laser designed with a 3.5 kW output is widely used to test the high-power laser performance of such fibers. Therefore, a 3.5 kW laser test platform with an MOPA structure was built, the schematic diagram of which is shown in Figure 9. The wavelength of the pumping source was 976 nm. In the experiment, the power of the 1080 nm seed light was 251 W, the length of gain of the fiber in the amplification stage was optimized to 14 m and the peak value of signal light increased with the increase in pump light power.
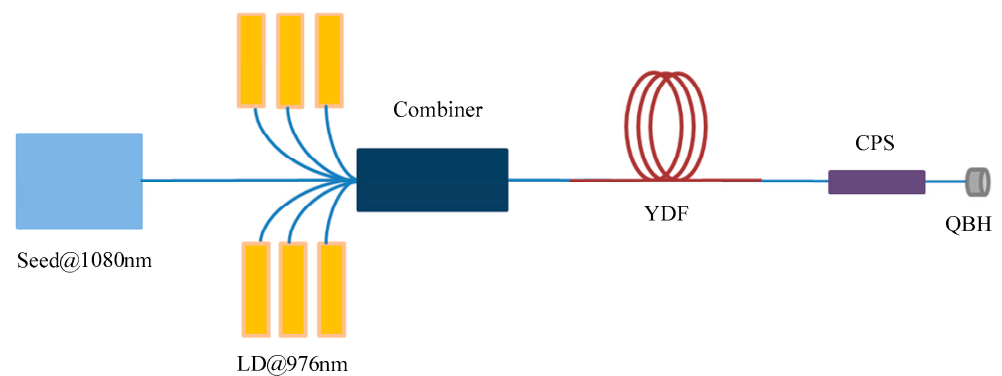
Figure 9. Schematic of 3.5 kW fiber laser system.

Figure 10 shows the variation in output power with pump power. It can be seen from the result that the output power increased linearly as the pump light power increased. The slope efficiency was 82.6%. When the pump injection power of the amplification stage reached 4025 W, the maximum laser output (3482 W) was obtained.
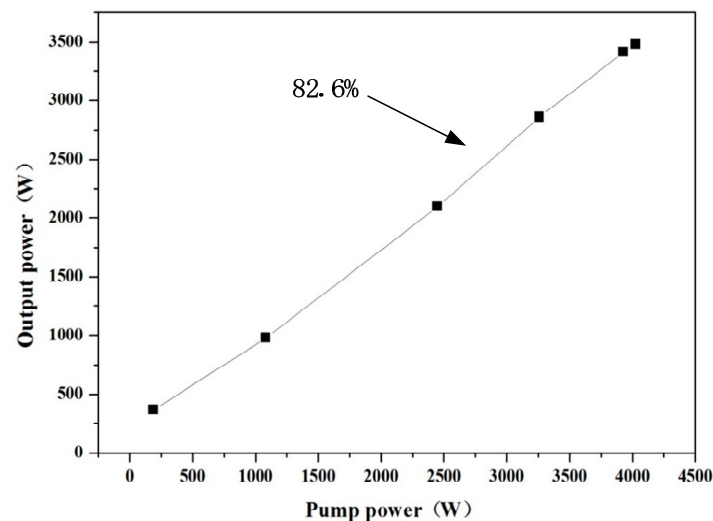

Figure 10. Relationship between pump power and output power.

This slope efficiency was higher compared with the slope efficiency of fiber before optimization (~79.8%). In order to explain the promotion of slope efficiency, the optical fields and energy distributions of the fundamental mode and high-order mode have been simulated (Figure 11). Through such simulation, we found that the transmission loss of the high-order mode was 5~10 times higher than that of the fundamental mode. For the laser generated in fibers with obvious dips in Yb ion concentration within the central area (Figure 3a), the concentration distribution matches more closely with the optical field of the high-order mode (Figure 11b) than the fundamental mode (Figure 11a). For the laser generated in a fiber with homogeneous concentration distribution (Figure 3b), the concentration distribution matches the optical field of the fundamental mode (Figure 11a). As a result, energy in the optimized sample is more concentrated on the fundamental mode with lower loss, which eventually leads to an increase in slope efficiency.
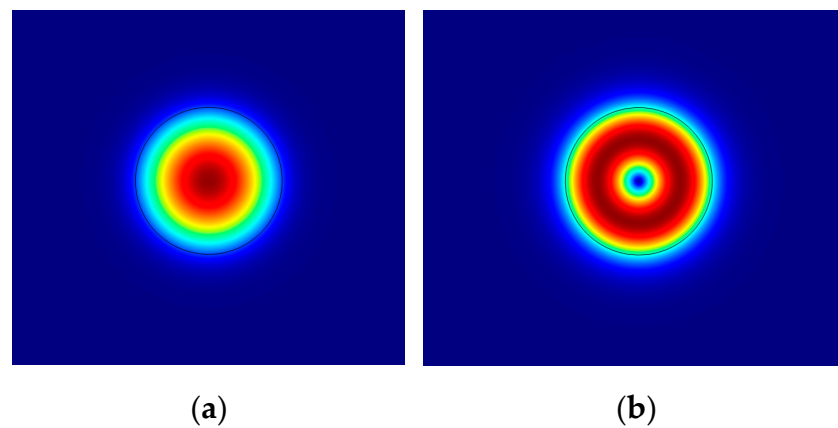
(**a**)　　　　　　　　　　(**b**)

Figure 11. Optical fields and energy distributions of (**a**) fundamental mode and (**b**) higher-order mode.

Figure 12 shows the spectrum of the output laser. The center wavelength of the output laser was 1080.1 nm. The linewidth of the output laser spectrum was 0.32 nm. There is no obvious intensity peak near the center wavelength, which demonstrates that no obvious Raman laser was generated from the nonlinear effect. The reduction in the nonlinear effect is because of the high nonlinear threshold. When the output power of the fiber is lower than the nonlinear threshold, there will be no nonlinear effect. In fiber with homogeneous Yb ion concentration distribution, the optical power distribution is uniform, and a homogeneous internal temperature distribution is achieved, which mitigates the accumulation of thermal effects and subsequent nonlinear effects. The stability of the 3.5 kW laser output power of a ytterbium-doped fiber was tested, as shown in Figure 13. After 8 h of continuous operation, the output power of the sample prepared in the experiment was maintained at 3480 W, and the value of power fluctuation was about 38 W.
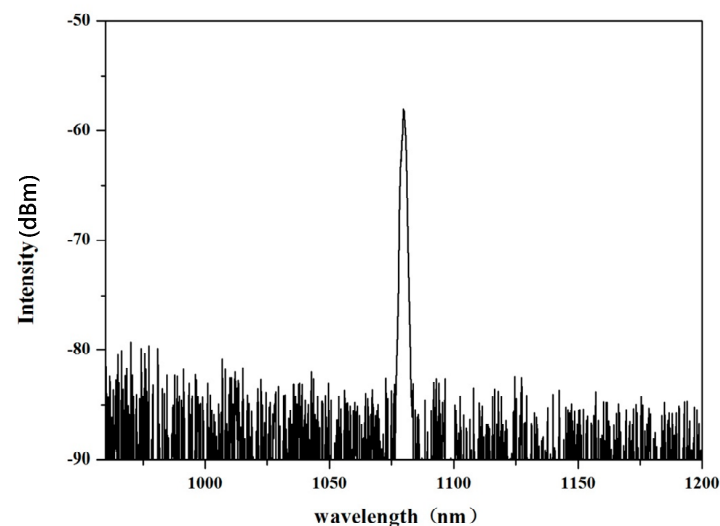

Figure 12. The output laser spectrum at 3.5 kW.

The experimental results presented above prove that the photodarkening effect in Yb-doped double-clad fiber operating at 3.5 kW was effectively suppressed. Combining this finding with previous results, we can confirm the suppression of the photodarkening effect when operating at both low output power and high output power in fiber with a greater uniformity of concentration distribution.
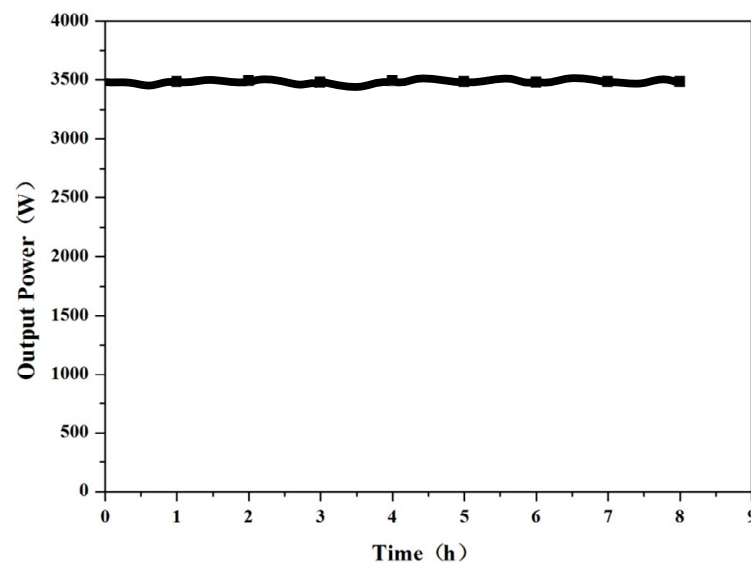
Figure 13. Power stability of 3.5 kW laser output in 8 h.

5. Conclusions

In this paper, ytterbium-doped double-clad fiber was obtained by the MCVD method combined with the CVD deposition process, and the doping uniformity of ytterbium ions in the core of the fiber was effectively improved by fine-tuning the proportion of the core glass components layer-by-layer through the technical process optimization. A 25/400 μm ytterbium-doped double-clad fiber with a top-flatten refractive index profile (RIP) was developed based on the fabricated fiber. The MOPA test system was built to achieve 3482 W laser output power under 4025 W pump power. No Raman effect was observed, and the laser continued to work for 8 h without noticeable output power reduction. By experimental study, it is proved that more attention should be paid to the uniformity of ytterbium ions doping in the fiber core, and the technology plays an important role in suppressing the PD effect, allowing for higher and stable output power.

Author Contributions: Conceptualization, Y.Y., P.G. and R.P.; methodology, Y.S., P.G. and R.P.; software, Y.S., S.X. and R.L.; validation, Y.S., P.G., S.X. and R.L.; formal analysis, Y.S.; investigation, S.X.; resources, Y.Y. and R.P.; data curation, Y.S., S.X. and R.L.; writing—original draft preparation, Y.S. and S.X.; writing—review and editing, P.G.; visualization, S.X. and R.L.; supervision, Y.Y., R.P. and R.L.; project administration, Y.Y.; funding acquisition, Y.Y. and P.G. All authors have read and agreed to the published version of the manuscript.

Institutional Review Board Statement: Not applicable.

Informed Consent Statement: Not applicable.

Data Availability Statement: Data can be provided upon request.

Conflicts of Interest: The authors are employed by the company China Electronics Technology Group Corporation. The authors declare that the research was conducted in the absence of any commercial or financial relationships that could be construed as a potential conflict of interest.

References

1. Richardson, D.J.; Nilsson, J.; Clarkson, W.A. High power fiber lasers: Current status and future perspectives. *JOSA B* **2010**, *27*, B63–B92. [CrossRef]
2. Yibo, W.; Jinyan, L. Status and development tendency of high power ytterbium doped fibers. *Chin. J. Lasers* **2017**, *44*, 0201009. [CrossRef]
3. Liu, C.P.; Liao, L.; Li, J.Y. Research progress on photodarkening of Yb-doped fiber lasers. *Lasers Optoelectron. Prog.* **2016**, *53*, 10–18.

4. Zervas, M.N.; Ghiringhelli, F.; Durkin, M.K.; Crowe, I. Distribution of photodarkening-induced loss in Yb-doped fiber amplifiers. In *Fiber Lasers VIII: Technology, Systems, and Applications*; SPIE: Bellingham, WA, USA, 2011; pp. 129–136.

5. Manek-Hönninger, I.; Boullet, J.; Cardinal, T.; Guillen, F.; Ermeneux, S.; Podgorski, M.; Doua, R.B.; Salin, F. Photodarkening and photobleaching of an ytterbium-doped silica double-clad LMA fiber. *Opt. Express* **2007**, *15*, 1606–1611. [CrossRef] [PubMed]

6. Li, N.; Yoo, S.; Yu, X.; Jain, D.; Sahu, J.K. Pump Power Depreciation by Photodarkening in Ytterbium-Doped Fibers and Amplifiers. *IEEE Photonic. Technol. Lett.* **2014**, *26*, 115–118. [CrossRef]

7. Otto, H.-J.; Modsching, N.; Jauregui, C.; Limpert, J.; Tünnermann, A. Impact of photodarkening on the mode instability threshold. *Opt. Express* **2015**, *23*, 15265–15277. [CrossRef] [PubMed]

8. Rybaltovsky, A.A.; Bobkov, K.K.; Velmiskin, V.V.; Umnikov, A.A.; Shestakova, I.A.; Guryanov, A.N.; Likhachev, M.E.; Bubnov, M.M.; Dianov, E.M. The Yb-doped aluminosilicate fibers photodarkening mechanism based on the charge-transfer state excitation. In *Fiber Lasers XI: Technology, Systems, and Applications*; SPIE: Bellingham, WA, USA, 2014; pp. 214–225.

9. Bobkov, K.K.; Rybaltovsky, A.A.; Vel'miskin, V.V.; Likhachev, M.E.E.; Bubnov, M.M.; Dianov, E.M.; Umnikov, A.A.; Gur'yanov, A.N.; Vechkanov, N.N.; Shestakova, I.A. Charge-transfer state excitation as the main mechanism of the photodarkening process in ytterbium-doped aluminosilicate fibres. *Quantum Electron.* **2014**, *44*, 1129. [CrossRef]

10. Engholm, M.; Norin, L. Preventing photodarkening in ytterbium-doped high power fiber lasers; correlation to the UV-transparency of the core glass. *Opt. Express* **2008**, *16*, 1260–1268. [CrossRef] [PubMed]

11. Lee, Y.; Sinha, S.; Digonnet, M.; Byer, R.; Jiang, S. Measurement of high photodarkening resistance in heavily Yb3+-doped phosphate fibres. *Electron. Lett.* **2008**, *44*, 14–16. [CrossRef]

12. Jelger, P.; Engholm, M.; Norin, L.; Laurell, F. Degradation-resistant lasing at 980 nm in a Yb/Ce/Al-doped silica fiber. *JOSA B* **2010**, *27*, 338–342. [CrossRef]

13. Engholm, M.; Jelger, P.; Laurell, F.; Norin, L. Improved photodarkening resistivity in ytterbium-doped fiber lasers by cerium codoping. *Opt. Lett.* **2009**, *34*, 1285–1287. [CrossRef] [PubMed]

14. Shao, C.; Ren, J.; Wang, F.; Ollier, N.; Xie, F.; Zhang, X.; Zhang, L.; Yu, C.; Hu, L. Origin of radiation-induced darkening in Yb3+/Al3+/P5+-doped silica glasses: Effect of the P/Al ratio. *J. Phys. Chem. B* **2018**, *122*, 2809–2820. [CrossRef]

15. Likhachev, M.E.; Aleshkina, S.S.; Shubin, A.V.; Bubnov, M.M.; Dianov, E.M.; Lipatov, D.S.; Guryanov, A.N. Large-mode-area highly Yb-doped photodarkening-free Al_2O_3-P_2O_5-SiO_2-based fiber. In *The European Conference on Lasers and Electro-Optics*; Optica Publishing Group: San Jose, CA, USA, 2011; p. CJ_P24.

16. Zhao, N.; Liu, Y.; Li, M.; Li, J.; Peng, J.; Yang, L.; Dai, N.; Li, H.; Li, J. Mitigation of photodarkening effect in Yb-doped fiber through Na+ ions doping. *Opt. Express* **2017**, *25*, 18191–18196. [CrossRef] [PubMed]

17. Sakaguchi, Y.; Fujimoto, Y.; Masuda, M.; Miyanaga, N.; Nakano, H. Suppression of photo-darkening effect in Yb-doped silica glass fiber by co-do** of group 2 element. *J. Non-Cryst. Solids* **2016**, *440*, 85–89. [CrossRef]

18. Fujimoto, Y.; Sugiyama, S.-I.; Murakami, M.; Nakano, H.; Sato, T.; Shiraga, H. Suppression mechanism by Ca additive of photodarkening effect in Yb-doped silica glass fiber. In *CLEO: Science and Innovations*; Optica Publishing Group: San Jose, CA, USA, 2013; CM4I. 6.

19. Mel'kumov, M.A.; Bufetov, I.A.; Kravtsov, K.S.; Shubin, A.V.; Dianov, E.M. Lasing parameters of ytterbium-doped fibers doped with P_2O_5 and $A1_2O_3$. *Quantum Electron.* **2004**, *34*, 843–848. [CrossRef]

20. Jetschke, S.; Unger, S.; Leich, M.; Kirchhof, J. Photodarkening kinetics as a function of Yb concentration and the role of Al codoping. *Appl. Opt.* **2012**, *51*, 7758–7764. [CrossRef]

21. Jetschke, S.; Unger, S.; Schwuchow, A.; Leich, M.; Jäger, M. Role of Ce in Yb/Al laser fibers: Prevention of photodarkening and thermal effects. *Opt. Express* **2016**, *24*, 13009–13022. [CrossRef] [PubMed]

22. Zhang, Z.; Luo, Y.; Xing, Y.; Li, H.; Peng, J.; Dai, N.; Li, J. Experimental comparison of Yb/Al/Ce and Yb/Al/P co-doped fibers on the suppression of transverse mode instability. *Front. Phys.* **2023**, *11*, 1124491. [CrossRef]

23. Engholm, M.; Tuggle, M.; Kucera, C.; Hawkins, T.; Dragic, P.; Ballato, J. On the origin of photodarkening resistance in Yb-doped silica fibers with high aluminum concentration. *Opt. Mater. Express* **2021**, *11*, 115–126. [CrossRef]

24. Bobkov, K.K.; Mikhailov, E.K.; Zaushitsyna, T.S.; Rybaltovsky, A.A.; Aleshkina, S.S.; Melkumov, M.A.; Bubnov, M.M.; Lipatov, D.S.; Yashkov, M.V.; Abramov, A.N.; et al. Properties of silica based optical fibers doped with an ultra-high ytterbium concentration. *J. Light. Technol.* **2022**, *40*, 6230–6239. [CrossRef]

25. Engholm, M.; Norin, L. Reduction of photodarkening in Yb/Al-doped fiber lasers. In *Fiber Lasers V: Technology, Systems, and Applications*; SPIE: Bellingham, WA, USA, 2008; pp. 303–310.

26. Mattsson, K.E. Low photo darkening single mode RMO fiber. *Opt. Express* **2009**, *17*, 17855–17861. [CrossRef] [PubMed]

27. Yang, Y.; Chu, Y.; Chen, Z.; Xing, Y.; Hu, X.; Li, H.; Peng, J.; Dai, N.; Li, J.; Yang, L. Blue up conversion in Yb^{3+}/Tm^{3+} co-doped silica fiber based on glass phase-separation technology. *Appl. Phys. A* **2018**, *124*, 1–6. [CrossRef]

28. Cao, R.; Yang, L.; Li, J.; Wang, Y.; Chen, G.; Zhao, N.; Xing, Y.; Liu, Y.; Lin, X.; Cheng, Y.; et al. Investigation of photo-darkening-induced thermal load in Yb-doped fiber lasers. *IEEE Photonics Technol. Lett.* **2019**, *31*, 809–812. [CrossRef]

29. Piccoli, R.; Robin, T.; Brand, T.; Klotzbach, U.; Taccheo, S. Effective photodarkening suppression in Yb-doped fiber lasers by visible light injection. *Opt. Express* **2014**, *22*, 7638–7643. [CrossRef] [PubMed]

30. Yoo, S.; Boyland, A.; Standish, R.; Sahu, J.K. Measurement of photodarkening in Yb-doped aluminosilicate fibers at elevated temperature. *Electron. Lett.* **2010**, *46*, 233–234. [CrossRef]

31. Zhao, N.; Li, W.; Li, J.; Zhou, G.; Li, J. Elimination of the photodarkening effect in an Yb-doped fiber laser with deuterium. *J. Light. Technol.* **2019**, *37*, 3021–3026. [CrossRef]
32. Yoo, S.; Basu, C.; Boyland, A.J.; Sones, C.; Nilsson, J.; Sahu, J.K.; Payne, D. Photodarkening in Yb-doped aluminosilicate fibers induced by 488 nm irradiation. *Opt. Lett.* **2007**, *32*, 1626–1628. [CrossRef]
33. Saha, M.; Pal, A.; Pal, M.; Guha, C.; Sen, R. An optimized vapor phase doping process to fabricate large core Yb-doped fibers. *J. Light. Technol.* **2015**, *33*, 3533–3541. [CrossRef]
34. Iho, A.; Söderlund, M.; i Ponsoda, J.M.; Koponen, J.; Honkanen, S. Modeling inversion in an ytterbium-doped fiber. In *Optical Components and Materials VI*; SPIE: Bellingham, WA, USA, 2009; Volume 7212, pp. 65–72.